Electronic Supplementary Material (ESI) for Sustainable Energy & Fuels.

Supplementary Materials for

High-performance Symmetry Flexible Solid-state Supercapacitors Induced by Methylene Blue with a Wide Voltage Window

Chunmei Xu, Haiyan Wang, Jiang Deng, and Yong Wang*

This PDF file includes:

Experiment section

1. Materials

Methylene blue ($C_{16}H_{18}ClN_3S \cdot 3H_2O$) and PVA (Polyvinyl Alcohol, molecular weight 89,000-98,000) were purchased from Aladdin, concentrated sulfuric acid was obtained from Sinopharm Chemical Reagent Co., Ltd. All chemicals without any further purification were analytical except MB was indicator. Commercial CC (carbon cloths, HCCP330) was purchased from Shanghai Hesen Electric Co. Ltd., China.

1.1 Synthesis of TCC

CC (4 *4 cm^2) was heated to 1000 ^oC in Nitrogen furnace for 1 h with a heating rate of 5 ^oC min^{-1} and the gas-flow rate was 250 mL min^{-1}, named as TCC_{1000}. After heating, TCC_{1000} was washed with deionized water and then dried for later use. The contrast sample was heated to 600 ^oC at the same conditions, named as TCC_{600}.

1.2 Assembly of the solid-state supercapacitors

2 g H_2SO_4 and 2 g PVA were added to 20 mL deionized water under continuously stirring, and then heated to 85 ^oC and mixed with a certain amount of MB until the solution became dark blue. The PVA-H_2SO_4 system was prepared as described above without adding MB. Two pieces of TCC and a piece of filter paper with area of 1 cm^2 were immersed into MB-PVA-H_2SO_4 electrolyte for an hour, then the filter paper was placed in between TCC just like sandwich. The whole thickness measured by vernier caliper was ~ 0.90 mm including two electrodes, separator and electrolyte. The whole mass of the positive and negative electrode was calculated to be about 26.5 mg.

2. Characterization

Scanning electron microscope (SEM) image was taken from Hitachi SU-70 microscope. The X-ray photoelectron spectra (XPS) used an aluminum anode (Al 1486.6 eV) X-ray source, collected with an ESCALAB MARK II spherical analyzer. The adsorption curve was characterized by UV-VIS Spectrophotometry (TU-1901). An ASAP 2020 V3.00H surface area and porosity analyzer was used to get Nitrogen adsorption−desorption isotherms and pore size distribution was calculated by the density functional theory (DFT) pore model.

3. Electrochemical Measurements

All the electrochemical tests were running at 25±1 ^{o}C. Cyclic voltammetry (CV) and electrochemical impedance spectroscopy (EIS) tests were tested on a Gamry Reference 600 electrochemical workstation. EIS was operated at open circuit potential with the amplitude 5 mV in the frequency range from 100 kHz to 0.01 Hz. Galvanostatic charge/discharge (GCD) was tested on Gamry Reference 600 (three electrode) and LAND CT2001A (two electrode), respectively. Liquid MB-1 M H_2SO_4 system and liquid 1 M H_2SO_4 were tested by three electrodes with TCC as working electrode, platinum sheet as the counter electrode, SCE electrode as reference electrode. The solid-state supercapacitors were measured by two electrodes.

4. Calculations

The following equations are used for calculating SCs performance:

Areal capacity (mF cm^{-2}), $$C_A = \frac{I \times t}{S \times \Delta V}$$

Volume capacity (mF cm^{-3}), $$C_V = \frac{I \times t}{V \times \Delta V}$$

Areal energy density (mW h cm^{-2}), $$E_A = \frac{C_A \times \Delta V^2}{2} \times \frac{1}{3600}$$

Volume energy density (mW h cm^{-3}), $$E_V = \frac{C_V \times \Delta V^2}{2} \times \frac{1}{3600}$$

Areal power density (mW cm^{-2}), $$P_A = \frac{E_A}{t}$$

Volume power density (mW cm^{-3}), $$P_V = \frac{E_V}{t}$$

Where I (A) is the current of discharge, t (s) is the discharge time, S represents the test area of electrode, ΔV (V) represents the voltage change of the test, and V (cm^{-3}) is the test volume of electrode.

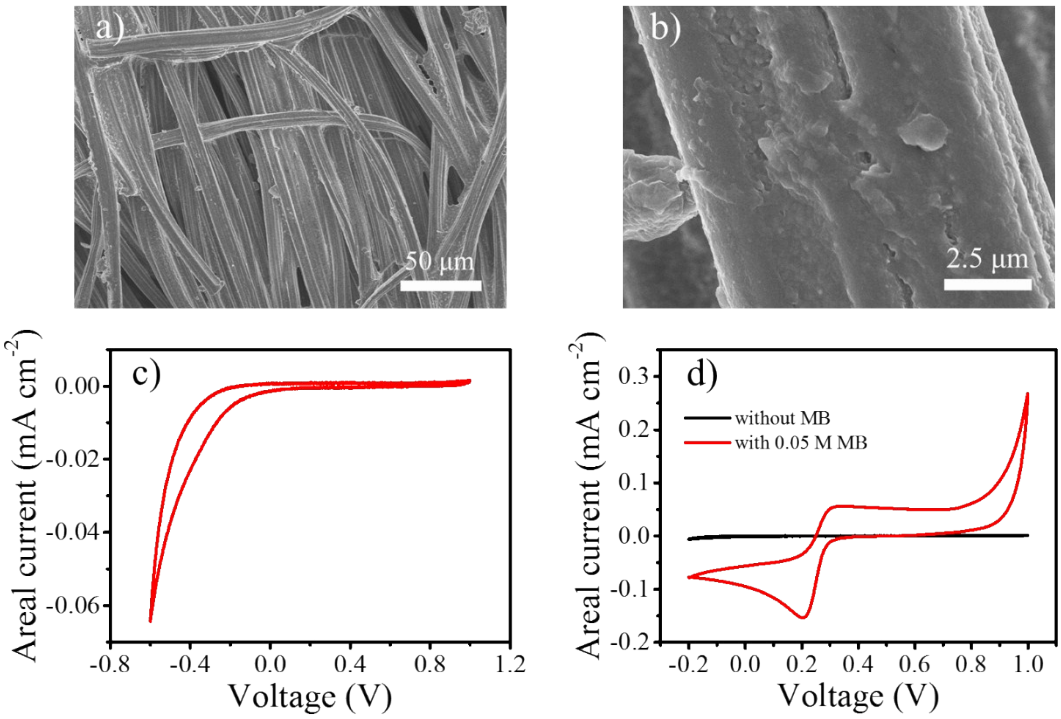

Figure S1. a) and b) SEM image of the CC. c) The CV curves of CC at -0.6 v-1 v in 1 M H_2SO_4 at 5 mv s^{-1}. d) The CV curves of CC in 1 M H_2SO_4 with or without MB at -0.2 v-1 v at 5 mv s^{-1}.

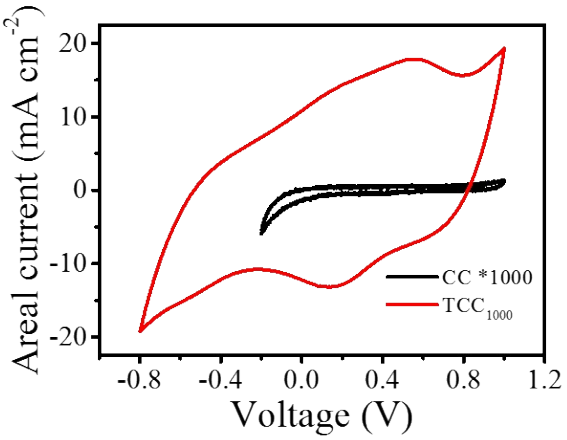

Figure S2. CV curves for CC (expanded for 500 times) and TCC_{1000} in 1 M H_2SO_4.

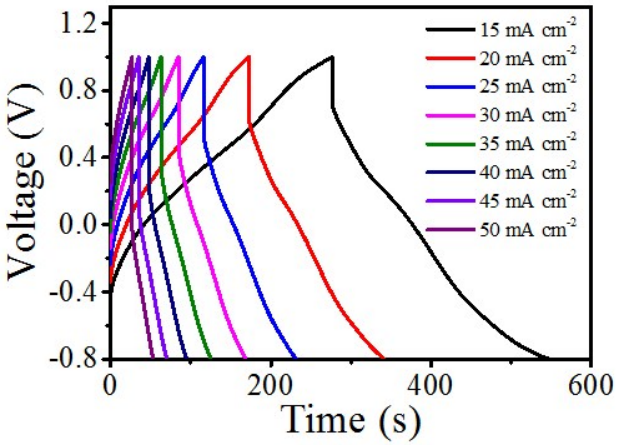

Figure S3. GCD curves for TCC_{1000} in 1 M H_2SO_4.

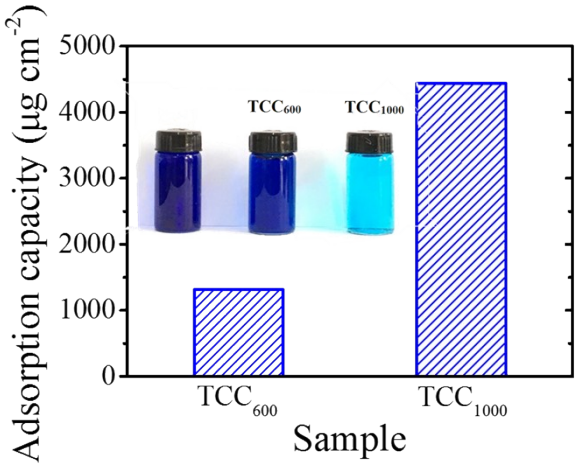

Figure S4. The adsorption capacity of TCC_x.

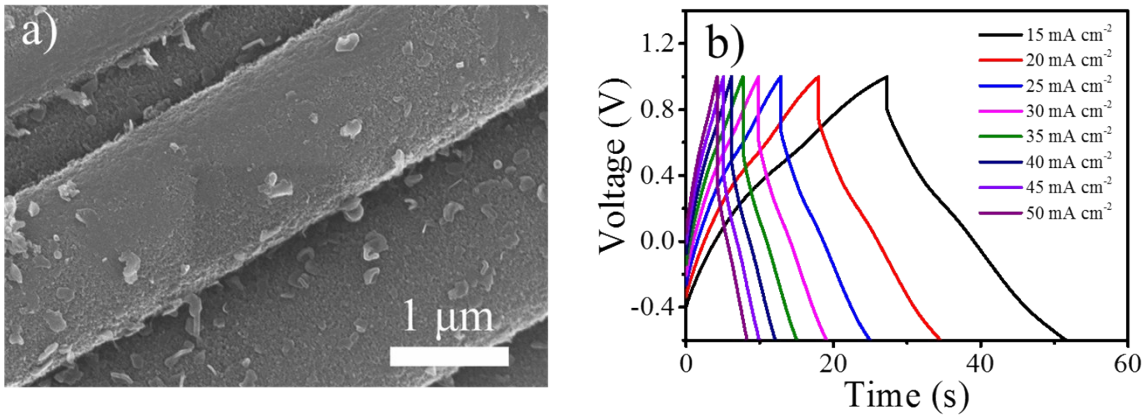

Figure S5. a) SEM image of the TCC_{600}. b) The GCD curves of TCC_{600} at -0.6-1 v in 1 M H_2SO_4 with 0.05 M MB. Because TCC_{600} with or without MB tested at -0.8-1 v occurred with hydrogen evolution reaction, we chose data tested at -0.6-1 v to compare with TCC_{1000}'s in the article.

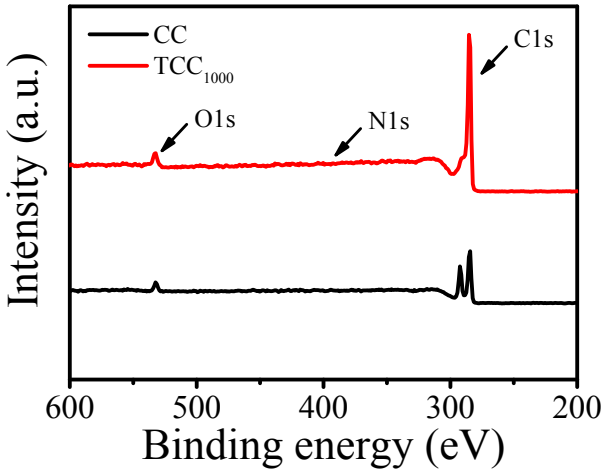

Figure S6. The XPS spectra of CC and TCC_{1000}.

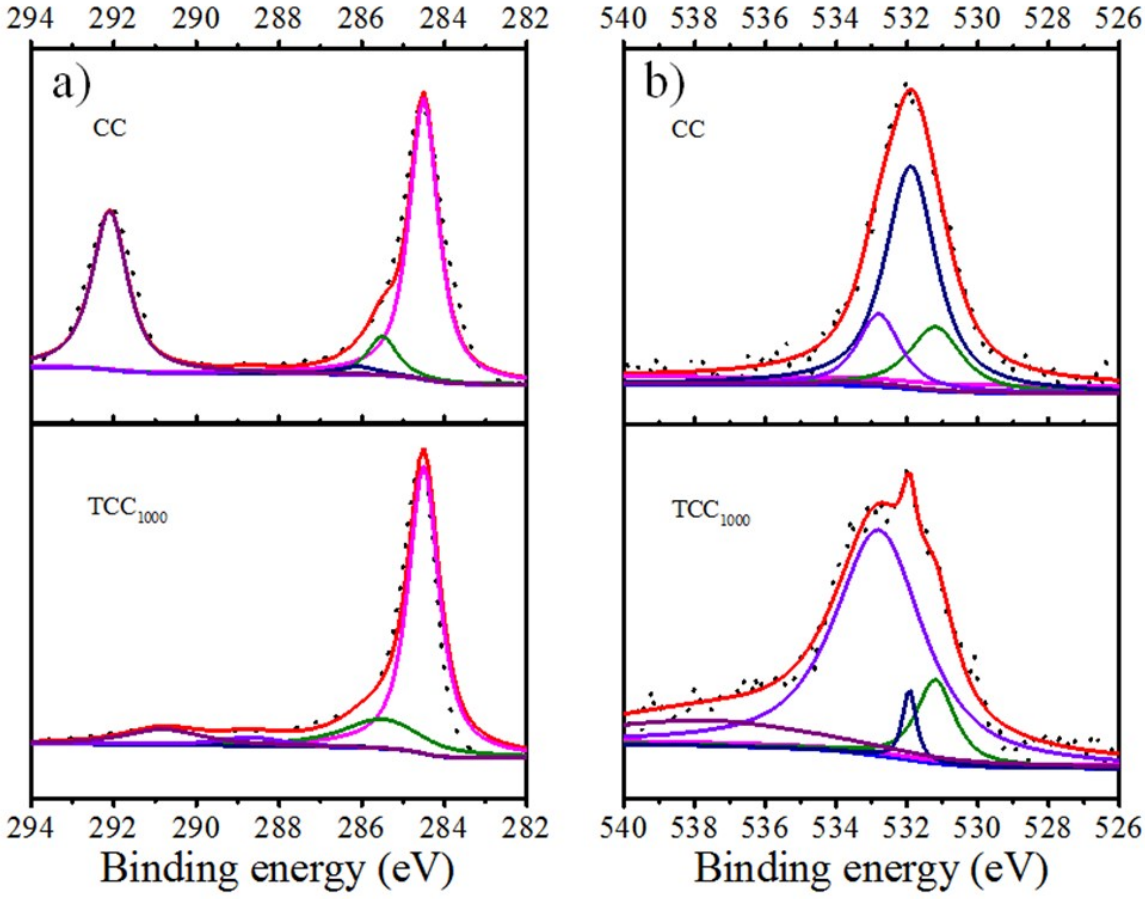

Figure S7. (a) The C1s and (b) O1s XPS fine scan spectrum of CC and TCC_{1000}.

Sample	C (at.%)	O (at.%)	C/O atom ratio	N (at.%)
CC	51.35	2.74	18.74	0
TCC_{1000}	93.54	4.86	19.25	1.61

Table S1. Summary of pore structure and elemental composition of CC and TCC_{1000}.

B.E. (eV)	C1 (284.5)	C2 (285.5)	C3 (286.1)	C4 (288.7)	C5 (290.8)	C6 (292.1)
Assignment	C=C	C-C	C-O	C(O)O	Graphitic shake-up	CF_3
CC	27.27	3.80	1.08	0.36	0	18.84
TCC_{1000}	63.98	16.74	0.19	3.84	8.79	0

Table S2. Fitted results (at. %) of C1s XPS spectra of CC and TCC_{1000}.

\

B.E. (eV)	O1 (530.5)	O2 (531.2)	O3 (531.9)	O4 (532.7)	O5 (533.5)
Assignment	Quinone	C(O)O	C=O	C-O	O-H
CC	1.71	0.19	0.64	0.18	0.02
TCC_{1000}	1.30	0.38	0.11	2.36	0.71

Table S3. Fitted results (at. %) of O1s XPS spectra of CC and TCC_{1000}.

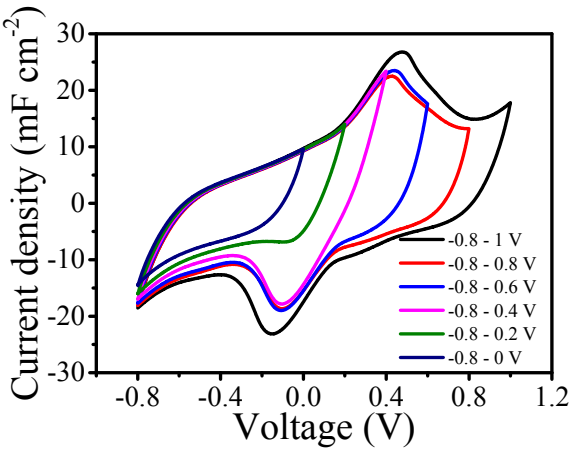

Figure S8. CV curves measured at different voltages at a scan rate of 5 mV s^{-1}.

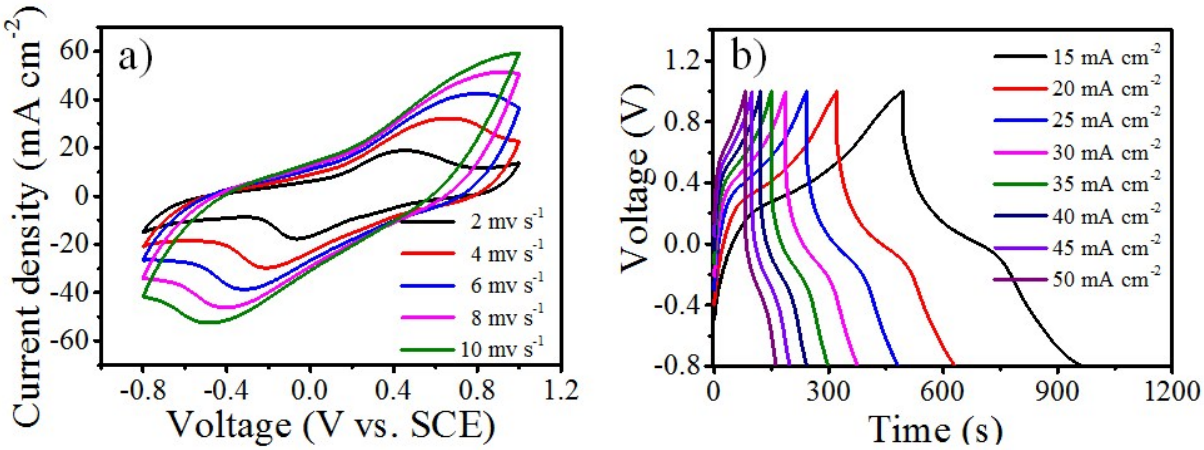

Figure S9. a) CV curves for TCC_{1000} in 1 M H_2SO_4 with 0.05 M MB. b) The GCD curves of 0.05 M MB at current densities from 15 to 50 mA cm^{-2}.

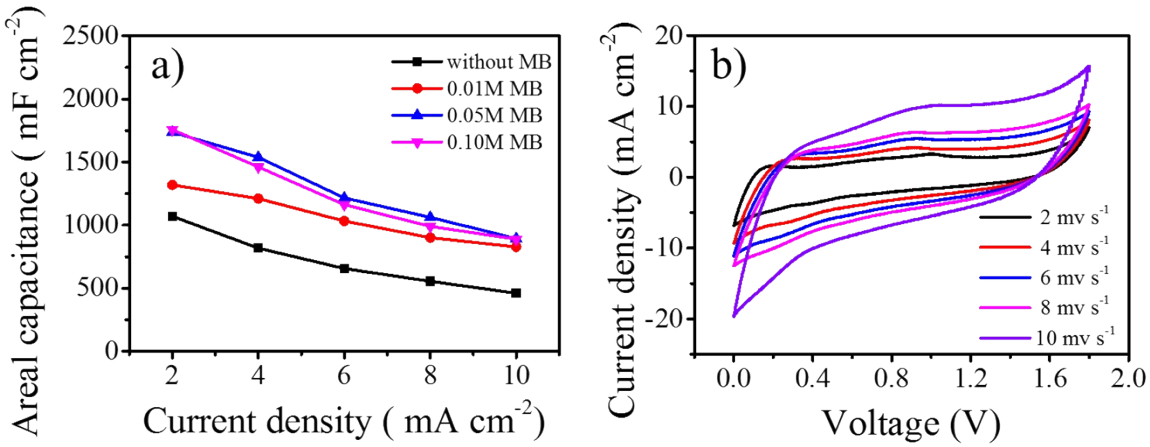

Figure S10. (a) Plots of the areal capacitance vs. current density for solid-state supercapacitors. (b) The CV curves of PVA-H_2SO_4 with 0.05 M MB at different scan rates.

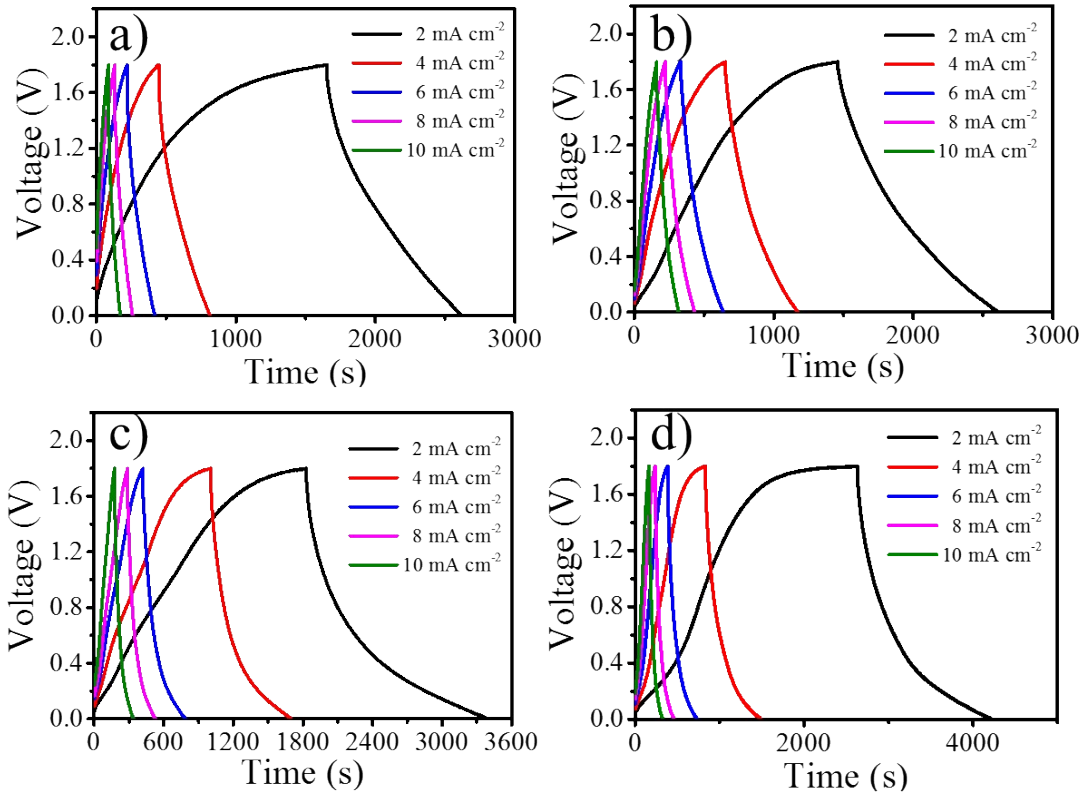

Figure S11. a) The GCD curves of solid-state SCs without MB. b) The GCD curves of solid-state SCs with 0.01 M MB. c) The GCD curves of solid-state SCs with 0.05 M MB. d) The GCD curves of solid-state SCs with 0.1 M MB.

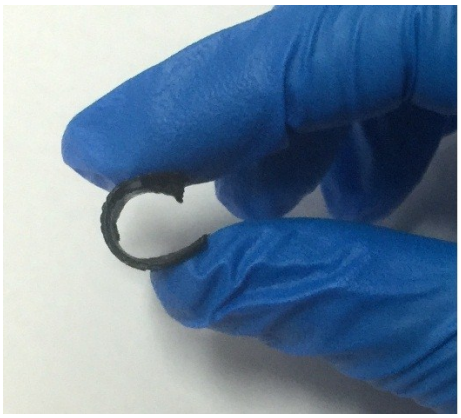

Figure S12. A digital photograph showed the flexibility of the device.

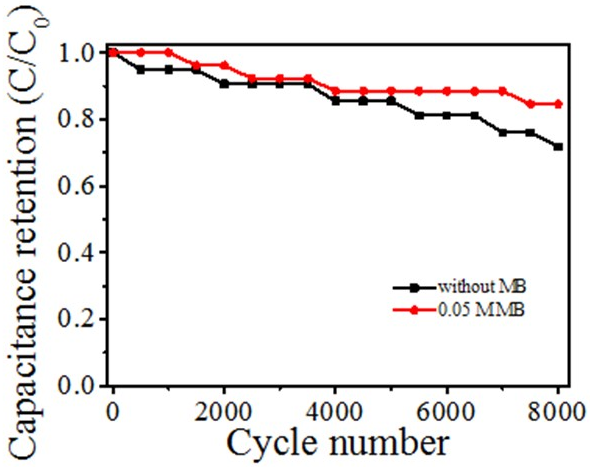

Figure S13. Cyclic life of PVA-H_2SO_4 with or without 0.05 M MB.

Electrolyte	Voltage	$E_{m,\ stack}$ (Wh/kg)	Cyclic stability	Ref
PVA-H_2SO_4-MB	1.8 V	29.4	8000 cycles (84.6%)	This work
PVA-H_2SO_4-IC	1.0 V	13.26	3000 cycles (80.3%)	1
PVA-H_2SO_4-bromamine acid sodium	1.5 V	30.5	1000 cycles (90%)	2
PVA-H_2SO_4-alizarin red S	1.6 V	39.4	1000 cycles (78%)	3
PVA-KOH-KI	1.0 V	7.80	1000 cycles (95.76%)	4
PVA-H_2SO_4–$VOSO_4$	1.0 V	12.83	——	5
PVA-KOH-$K_3[Fe(CN)_6$	1.0 V	57.94	1000 cycles (98.3%)	6
PVA-H_2SO_4-KI-$VOSO_4$	0.8 V	25.4	3000 cycles (93.7%)	7
PVA-H_2SO_4-HQ-PPy	0.8 V	4.7	2000 cycles (103%)	8
PVA–H_2SO_4–p-benzenediol	1 V	11.31	——	9
PVA–H_2SO_4–PySH	0.8 V	——	1000 cycles (88 %)	10
PVA–H_2SO_4–$VOSO_4$	1 V	7.7	——	11
PVA/H_3PO_4/Na_2MoO_4	1 V	——	2500 cycles	12
PEDOT/Fc	1.5 V	27.4	3000 cycles (75%)	13
PEDOT/Fc/4-oxo-TEMPO	1.5 V	20.8	3000 cycles (89%)	13

Table S4. Comparison of the electrochemical performance of solid-state SCs with 0.05 M MB in this work with other additives solid-state SCs reported in previous reports.

References

(1). G. Ma, M. Dong, K. Sun, E. Feng, H. Peng and Z. Lei, J. Mater. Chem. A, 2015, 3, 4035-4041.

(2). E. Feng, Feitian Ran, Ziqiang Lei., New J. Chem., 2016, DOI: 10.1039/c6nj02710e.

(3). K. Sun, F. Ran, G. Zhao, Y. Zhu, Y. Zheng, M. Ma, X. Zheng, G. Ma and Z. Lei, Rsc Adv., 2016, 6, 55225-55232.

(4). H. Yu, J. Wu, L. Fan, K. Xu, X. Zhong, Y. Lin and J. Lin, Electrochim. Acta, 2011, 56, 6881-6886.

(5). S. T. Senthilkumar, R. K. Selvan, N. Ponpandian, J. S. Melo and Y. S. Lee, J. Mater. Chem. A, 2013, 1, 7913-7919.

(6). G. Ma, J. Li, K. Sun, H. Peng, J. Mu and Z. Lei, J. Power Sources, 2014, 256, 281-287.

(7). L. Q. Fan, J. Zhong, J.-H. Wu, J.-M. Lin and Y.-F. Huang, J. Mater. Chem. A, 2014, 2, 9011-9014.

(8). R. Xu, F. Guo, X. Cui, L. Zhang, K. Wang and J. Wei, J. Mater. Chem. A, 2015, 3, 22353-22360.

(9). H. Yu, J. Wu, L. Fan, Y. Lin, K. Xu, Z. Tang, C. Cheng, S. Tang, J. Lin and M. Huang, J. Power Sources, 2012, 198, 402-407.

(10). S. Pan, J. Deng, G. Guan, Y. Zhang, P. Chen, J. Ren and H. Peng, J. Mater. Chem. A, 2015, 3, 6286-6290.

(11). L. Q. Fan, J. Zhong, C. Y. Zhang, J. H. Wu and Y. L. Wei, Int. J. Hydrogen Energy, 2016, 41, 5725-5732.

(12). G. K. Veerasubramani, K. Krishnamoorthy, P. Pazhamalai and J. K. Sang, Carbon, 2016, 105, 638-648.

(13). H. Zhang, J. Li, C. Gu, M. Yao, B. Yang, P. Lu and Y. Ma, J. Power Sources, 2016, 332, 413-419.